




ORIGINAL RESEARCH

Open Access



High-resolution wildfire simulations reveal complexity of climate change impacts on projected burn probability for Southern California

Alex W. Dye^{1*†} , Peng Gao^{2†}, John B. Kim³, Ting Lei⁴, Karin L. Riley⁵ and Larissa Yocom⁶

Abstract

Background Wildfire is a major contemporary socio-ecological issue facing the people and natural resources of Southern California, and the prospect that a warming climate could lead to a higher probability of fire in the future is cause for concern. However, connecting climate change to projected burn probability is complex. While most models generally show temperature increasing in the future, changes in humidity and precipitation are less certain, and these changes interact to generate projections of future climates that are sometimes, but not always, more conducive to wildfire. We ran FSim, a stochastic, high-resolution spatial (270 m) and temporal (daily) fire spread model, with projected Energy Release Component (ERC) derived from multiple global climate models (GCMs) under RCP8.5 climate change scenario to explore the impact of a range of future climate trajectories on simulated burn probability and to quantify the uncertainty arising from multiple GCMs.

Results We observed considerable uncertainty in the future direction of change for burn probability. Future changes were more certain in the Southern Coast region of California, where 75% of simulations projected an increase in burn probability. In the Central Coast region, five out of eight GCM-based simulations projected increased burn probability. Less than 1% of the total burnable study area had unanimous agreement on the projected direction of change. Simulated changes in burn probability were directly correlated to annual projections of changes in ERC, but were also affected by the seasonality of ERC change, as well as interactions between humidity, precipitation, and temperature.

Conclusions The observed variability offers insights into why, and under what climate conditions, burn probability may increase or decrease in the future. Our study is novel in its examination of a wide range of potential future burn probability projections for Southern California using a regional application of a high-resolution stochastic fire spread model, and the complexity that we demonstrated for Southern California suggests that simple correlations of increasing fire with increasing temperature are likely underestimating the range of plausible future fire scenarios.

Keywords FSim, Climate change, California, Wildfire modeling, Burn probability, Energy release component (ERC), Western United States

[†]Alex W. Dye and Peng Gao contributed equally to first-authorship of this manuscript

*Correspondence:

Alex W. Dye
alex.dye@oregonstate.edu

Full list of author information is available at the end of the article



Resumen

Antecedentes Los incendios de vegetación constituyen uno de los mayores problemas que afectan a las personas y los recursos naturales del sur de California, y la proyección de que el calentamiento del clima podría llevar a mayores probabilidades de incendios en el futuro es motivo de preocupación. Sin embargo, la conexión del cambio climático con la probabilidad esperada de incendios a futuro es compleja. Mientras que la mayoría de los modelos generalmente muestran temperaturas que se incrementan en el futuro, los cambios en la humedad y la temperatura son menos ciertos, y estos cambios interactúan para generar proyecciones de climas futuros que son algunas veces, aunque no siempre, más conducentes a fuegos de vegetación. Nosotros hicimos correr el FSim, un modelo de propagación del fuego estocástico y de resolución espacial (270 m) y temporal (diario), con un Componente Proyectado de Liberación de Energía (ERC por sus siglas en inglés), derivado de múltiples modelos del clima global (GCMs) bajo el escenario de cambio climático RCP8.5. Esto fue hecho para explorar el impacto de un rango de futuras trayectorias del clima en probabilidades de fuegos simulados y para cuantificar la incertidumbre que proviene de múltiples GCMs.

Resultados Observamos una gran incertidumbre en la futura dirección del cambio en la probabilidad de ocurrencia de incendios. Los cambios futuros fueron más seguros en la región de la costa sur de California, en donde el 75% de las simulaciones proyectaron un incremento en la probabilidad de incendios. En la región de la costa central, cinco de un total de ocho simulaciones basadas en GCMs proyectaron un incremento en la probabilidad de incendios. Menos del 1% del total del área de estudio con probabilidad de quemarse presentó un acuerdo unánime en la dirección de los cambios proyectados. Los cambios simulados en la probabilidad de incendios estuvieron directamente correlacionados a las proyecciones anuales de cambios en ERC, pero estuvieron también afectados por la estacionalidad del cambio ERC, como también en las interacciones entre humedad, precipitación y temperatura.

Conclusiones La variabilidad observada permite conocer el porqué, y bajo qué condiciones de clima, las probabilidades de incendio pueden aumentar o disminuir en el futuro. Nuestro estudio es novedoso en la exploración dentro un rango amplio de proyecciones potenciales de futuras probabilidades de incendios para el sur de California, utilizando una aplicación regional de un modelo de propagación del fuego estocástico y de alta resolución. La complejidad que nosotros demostramos para el sur de California sugiere que las correlaciones simples del incremento del fuego con el aumento de las temperaturas están probablemente subestimando el rango de posibles escenarios de fuego futuros.

Background

Climate change is one of the major factors linked to increased wildfire activity in the Western U.S., including Southern California (Diffenbaugh et al. 2015; Abatzoglou and Williams 2016; Williams et al. 2019; Goss et al. 2020). Environmental conditions conducive to wildfire, including higher temperatures, drought, and a longer fire season, may continue to intensify through the end of the twenty-first century (Batllori et al. 2013; Barbero et al. 2015; D. McEvoy et al. 2020a, b; Brown et al. 2021; Ma et al. 2021; Dong et al. 2022). In particular, extreme drought may increase substantially in California (Cook et al. 2015; D. McEvoy et al. 2020a, b; Brey et al. 2021), and earlier spring warming and later autumn cooling are expected to compress the winter rainy season and extend the summer dry season conducive to wildfires (Westerling 2016; Luković et al. 2021; Swain 2021). In the absence of changes in precipitation and humidity, rising temperatures would raise vapor pressure deficit and evapotranspiration, accelerating

drying and increasing the flammability of fuels (Williams et al. 2013).

Predicting the future of wildfire in California is not simple or clear, however. Although there is broad agreement among climate models that point towards hotter futures for Southern California (Cook et al. 2015; Diffenbaugh et al. 2015), precipitation quantity and timing are more uncertain, complicating projections of fuel moisture, an important parameter for assessing fire activity (Neelin et al. 2013; Swain et al. 2018). Even when an overall drier future is projected, enhanced variability in seasonal extremes can lead to increases in both very wet and very dry years (Swain et al. 2018). For Southern California, D. McEvoy et al. (2020a, b) showed that 7 global climate models (GCM) unanimously projected a future increase in the average number of days per summer above the 95th percentile of the Evaporative Demand Drought Index (EDDI), but the magnitude varied by as much as 30 days per summer between individual GCMs. Factors like the magnitude, seasonality, and spatial variability of

projected climate changes have proven critical to making connections with future fire activity. For example, Westerling and Bryant (2008) examined statistical models to show that burn probability could either increase or decrease by as much as 30% by 2100 in California, while Lenihan et al. (2008) used simulations from a dynamic vegetation model to show that annual area burned could either increase by as much as 50% or decrease by 40%. Seasonal variation is particularly important for linking climate to fire in Southern California, where the fire season is long and often extends beyond the hot, dry summer season into the autumn, where fire growth can be exacerbated by fast, dry winds, such as the Santa Ana or Diablo winds (Jin et al. 2014; Faivre et al. 2016; Keeley et al. 2021).

Because of this complexity, several modeling approaches have been used to explore the relationship between climate change and wildfire in California. Statistical models have extrapolated contemporary regression relationships between climate and fire into the future (Liu et al. 2013; Brown et al. 2020; Goss et al. 2020; Gannon et al. 2021; Dong et al. 2022), and while statistical models have computational efficiency and the ability to be applied to a large area, they lack representation of the spatial processes of wildfire, including fire spread and containment. Statistical models mostly depend on correlations between monthly climate means and area burned; these correlations do not tend to be strong and miss critical factors like daily sequencing of weather and its effect on fire spread across topographically complex landscapes. Fire behavior and spread models can accomplish this task, but are more often applied to small areas because of their computational cost and the complexity of model calibration (Clark et al. 2008; Peterson et al. 2011; Zigner et al. 2020). Models such as FlamMap (Finney 2006) and FARSITE (Finney 2004) require the user to specify weather and fuel moisture conditions, and therefore cannot account for the probability of various sequences of ignition and weather.

The large-fire simulator FSim is a wildfire model that combines the strengths of statistical models with spatially explicit wildfire simulation models (Finney et al. 2011). FSim simulates ignition, spread, and containment of wildfires on a fine-scale gridded landscape (generally 90–270 m cells). FSim simulates the ignition and growth of wildfires under tens of thousands of hypothetical fire seasons to estimate the probability of a given area burning under modeled landscape conditions and has been widely used to develop national (Finney et al. 2011) and regional maps of contemporary wildfire probability in California and elsewhere (Scott et al. 2012, 2017; Thompson et al. 2013; Riley et al. 2018; Vogler et al. 2021). FSim has been integrated with climate change projections to

assess future burn probability in two limited areas: northern Idaho (Riley and Loehman 2016) and northwestern Oregon (A. McEvoy et al. 2020a, b).

In this paper, we describe an application of FSim to the coastal region in Southern California, spanning San Francisco to the Mexican border (Fig. 1), to create maps of mid-twenty-first century burn probability at 270 m resolution. The 12 345 km² study area comprises some of the most densely populated portions of California. These areas also have high ecological (Myers et al. 2000) and economic importance (Srivastava et al. 2020) and a recent history of high-impact wildfires. To our knowledge this is the first application of the high-resolution wildfire simulation model FSim to Southern California that incorporates multiple future GCM-based climate projections to produce high-resolution maps of future wildfire probabilities. The ensemble of FSim outputs we generated have the potential to serve as a basis for exploring how a wide range of future climate change projections under the RCP8.5 emissions scenario may create various spatial patterns of burn probabilities, as well as to invigorate and challenge fire modeling methodologies under climate change.

Methods

Study area

We applied FSim to the region spanning the Southern California coast from San Francisco to the Mexico border (Fig. 1) for two adjacent pyromes, or areas of relatively homogenous fire regime defined by fire size, frequency, intensity, and seasonality (Short et al. 2020). Pyrome 33 (henceforth Central Coast) extends south from the southern tip of San Francisco Bay, including the coast range and extending east to the edge of the Central Valley. Elevation ranges from sea level to over 1500 m, and the climate is Mediterranean with mild, wet winters and hot, dry summers. The vegetation is predominantly chaparral and coastal sage scrub, with some woodlands and forests at higher elevations. Intense downslope winds occur seasonally in this region but are more frequent in the southern half of the pyrome (Dye et al. 2020). In the northern half of the pyrome, agriculture dominates the valleys. Several large cities are located along the coast in this pyrome, including Santa Maria, San Luis Obispo, and Santa Barbara, with extensive suburbs and exurbs surrounding them creating wildland-urban interface (WUI).

Pyrome 34 (henceforth Southern Coast) extends from the Santa Monica Mountains northwest of Los Angeles to San Diego and the US-Mexico border. The pyrome includes multiple high-elevation mountain ranges with several peaks rising above 3000 m and extends to the edge of the deserts to the north and to the east. The

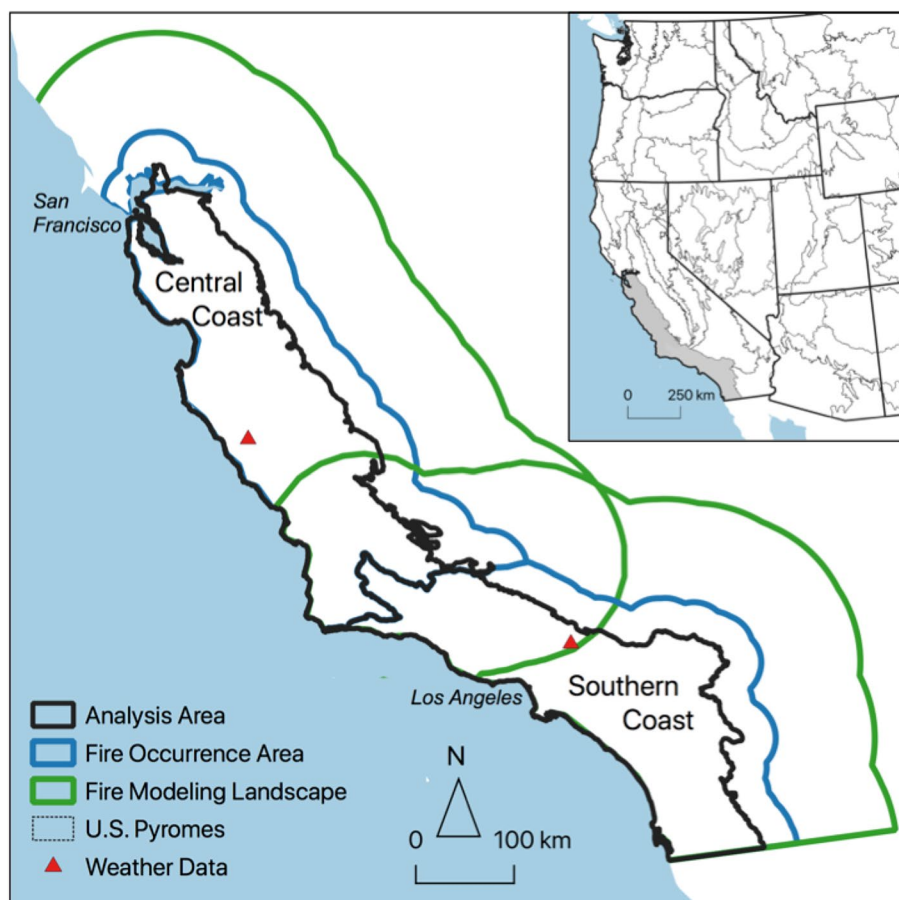


Fig. 1 The study area of Southern California describing spatial boundaries used for FSim modeling, including the locations selected for weather data in each pyrome. Inset map shows the division of pyromes across the Western United States

climate in this pyrome is also Mediterranean. Rainfall occurs primarily in the winter, with the interior parts of the pyrome receiving less than the coast. Although the vegetation is predominantly chaparral and coastal sage scrub, the mountain ranges also support forests and woodlands. Many of the largest fires are driven by Santa Ana winds, and occur in the fall (Keeley et al. 2021). Several statistical studies have projected future increases in fire size and frequency in this region (Barbero et al. 2015; Madadgar et al. 2020; Brey et al. 2021; Brown et al. 2021; Gao et al. 2021), and it has experienced several large, high-consequence contemporary wildfires (Keeley et al. 2009; Nauslar et al. 2018; Keeley and Syphard 2021).

The large fire simulator (FSim)

FSim is described in detail in other publications (e.g. Finney et al. 2011; Scott et al. 2012; Thompson et al. 2013; Riley and Loehman 2016), and here we summarized only its key features relevant to our study. FSim is a stochastic, spatially explicit model that incorporates

weather, topography, fuels, and spatial patterns of historical ignition probability to model the ignition and spread of fires. FSim computes a daily large-fire ignition probability based on the logistic regression between historical large fire ignitions in the study area and the daily Energy Release Component (ERC) for fuel model G of the National Fire Danger Rating System (Andrews et al. 2003; Finney et al. 2011). ERC is a proxy for fuel dryness, and incorporates daily temperature, precipitation duration, humidity, and state of the weather (SOW) (Cohen and Deeming 1985). FSim only ignites and spreads fires on days where ERC equals or exceeds the 80th percentile ERC for that region (hereafter, these days are referred as “burn days”) (Table 1), a threshold considered to demarcate the fire season based on the relationship between large fire ignitions and ERC across most of the contiguous United States (Riley et al. 2013).

During a full simulation of a specific climate period (e.g. 1992–2015), FSim generates statistically plausible weather streams for tens of thousands of iterations of the

Table 1 Fire statistics for observational records in each pyrome over the contemporary calibration period (1992–2015). Average fire size and frequency statistics are from the Short (2017) database. The 80th % ERC threshold is calculated from ERC values for the gridMET pixel coinciding with the Fort Hunter Liggett RAWS (Central Coastal) and the Chilao RAWS (Southern Coastal)

	Area (km ²)	Average fire size (km ²) [70% confidence interval]	Fire Frequency (per year per 10 ³ km ²) [70% confidence interval]	80 th % ERC
Central Coastal	76 890.27	8.54 [7.16, 9.11]	0.43 [0.41, 0.45]	58.6
Southern Coastal	50 261.96	14.12 [12.38, 15.86]	0.87 [0.84, 0.91]	83.6

same hypothetical calendar year. On each day of the year, FSim randomly draws a wind speed and direction value from their monthly joint probability distribution for the period being simulated. Daily ERC values are generated based on the mean ERC value for that day in the weather records for the period of study, the standard deviation in ERC for the day, and the temporal autocorrelation in ERC. Using this method, any number of years of synthetic ERC streams can be simulated, with a typical number of years for this part of the country being 10,000. If the ERC value selected meets the 80th percentile threshold, FSim can ignite new fires and/or spread existing fires. Locations of new ignitions are determined probabilistically using a continuous kernel density raster supplied by the user (in our study, we used a 40-km nearest neighbor) that represents the spatial point pattern of historical ignition locations (Short 2017). A single iteration begins on January 1 and is completed once FSim reaches December 31. At this point, all existing fires, if any, are ended, and the next independent iteration year begins on January 1. Iterations are not sequential or temporally related. By performing tens of thousands of these iterations, FSim produces stable and repeatable estimates of burn probability for any given location on the simulation landscape. Model outputs include ignition location, date, final size, and perimeter of each simulated fire. FSim focuses on modeling only large fires to maintain computational efficiency, and because large fires account for the vast majority of area burned. Following Scott (2014), we used a large-fire threshold of 404.686 km² (100 acres) for our study. Henceforth, all of our reported results are based on fires at or above this large-fire threshold.

FSim requires specification of three spatial boundaries for each pyrome being modeled (Fig. 1). The “analysis area” is the primary region of interest and the area for which final burn probability estimates are valid, equaling the areas of the Central Coast and Southern Coast

pyromes. The “fire occurrence area” (FOA) defines where FSim allows ignitions to start by probabilistically assigning ignition locations using a continuous kernel density raster representing the spatial point pattern of historical ignition locations (Short 2017). We set the FOA as a 30 km buffer around each pyrome, but did not buffer the border between the two pyromes so that fires could spread between the pyromes without being counted multiple times (Thompson et al. 2013). Third, FSim requires a “fire modeling landscape” (LCP) raster, which we set as a 60 km buffer surrounding the FOA. FSim does not allow ignitions in this buffer, but fires ignited in the FOA can burn outward through the LCP, preventing edge effects that might otherwise occur if fire spread was forced into a hard boundary. We acquired spatial landscape inputs of slope, elevation, aspect, fire behavior fuel model (Scott and Burgan 2005), canopy bulk density, canopy base height, canopy cover, and canopy height from the Landscape Fire and Resource Management Planning Tools, or LANDFIRE, 2016 Remap (LANDFIRE 2018). We used LANDFIRE products off-the-shelf, following standard FSim procedures (Finney et al. 2011), and did not conduct additional local calibration of fuel models or canopy characteristics. LANDFIRE’s canopy layers are internally calibrated for use with the Scott and Reinhardt (2001) crown fire model, which is used in FSim. We resampled the default LANDFIRE 30 m raster grids to 270 m to match our desired output resolution, then combined all eight grids using standard tools in FlamMap software (Finney 2006) to create the LCP raster required for FSim.

Modeling protocol

When referencing our modeling protocol, we have adopted the following terminology: a climate scenario refers to the historical, contemporary, or future (under RCP8.5 emissions trajectory) climate time periods; a climate projection refers to a unique representation of a scenario (e.g. a projection of the 2040–2069 future climate scenario for a selected GCM); and a simulation refers to a 10,000 iteration run of the FSim model informed by climate data from a unique projection of a climate scenario. We defined four climate scenarios to model: contemporary calibration (1992–2015), baseline (1979–2005), historical (1979–2005), and future (2040–2069) (Table 2).

Contemporary calibration (1992–2015)

The contemporary calibration scenario (1992–2015) was included for the purpose of calibrating FSim, because this period best corresponds with the available observed fire records (Short 2017). Following standard FSim best practices, we calibrated FSim until both the mean fire size and mean number of fires per year were each within the 70%

Table 2 Summary of the different simulation scenarios and their purpose within our modeling framework

Scenario	Climate Data	Purpose
Contemporary Calibration (1992–2015)	gridMET	Calibrate model settings to reflect observed contemporary fire statistics
Baseline (1979–2005)	gridMET	Simulations covering historical GCM period for comparison with GCM-based simulations
Historical (1979–2005)	8 GCMs (downscaled MACAv2-METADATA)	GCM-based simulations for the historical period
Future (2040–2069)	8 GCMs (downscaled MACAv2-METADATA)	GCM-based simulations for mid-twenty-first century under RCP8.5 emissions

confidence intervals of the 1992–2015 observed means (Table 1).

We supplied FSim with ERC data derived from gridMET, an observation-based gridded climate dataset that blends spatial attributes of the gridded climate data Parameter-elevation Relationships on Independent Slopes Model (PRISM) (Daly et al. 2008) with desirable temporal attributes from regional reanalysis using climatically aided interpolation (Abatzoglou 2013). We used Fire Family Plus (Bradshaw and McCormick 2009) to calculate daily ERC from gridMET. Since ERC calculations required a state of weather (SOW) variable that is not included in gridMET, we calculated SOW from gridMET precipitation duration and percent of cloud cover, where cloud cover was inferred from the ratio between solar radiation and potential maximum radiation, and we calculated precipitation duration following methods described by Abatzoglou and Kolden (2013).

Conventionally, FSim is driven with weather data from a single representative weather station within the pyrome. For this study, we identified a Remote Access Weather Station (RAWS) with a relatively central location within each pyrome and with long, complete wind records. In the Central Coast, we chose the Fort Hunter Liggett RAWS (36° 00' 42" N, 121° 14' 30" W), and in the Southern Coast we chose the Chilao RAWS (34° 19' 54" N, 118° 01' 49" W). The wind speed and direction distribution tables required by FSim were constructed from RAWS because spatially downscaled wind data in gridMET may poorly represent the wind patterns at the selected RAWS locations. ERC values for 1992–2015 were taken from the gridMET pixel that coincided with the RAWS coordinates (Fig. 1).

Calibration consisted primarily of adjusting three model parameters in FSim: the rate of spread multipliers, “acrefract” (a divisor number that FSim applies to help model the probability of a large fire day), and the wind speed distribution table. In FSim, wind speed bins are typically capped at 30mph. Even though we could successfully calibrate to annual statistics without changing

the default wind speed bins, we simulated lower than expected fire sizes during the Santa Ana wind season, Oct-Dec (Raphael 2003). Since the Santa Ana winds routinely exceed 30 mph, we manually adjusted the wind speed distributions to allow for winds up to 100 mph that were recorded in the historical observations. This had the desired effect of increasing average fire size in the fall and winter. To isolate the effect of climate change, and following the approach of Riley and Loehman (2016) we retained the LCP raster, the ignition probability grid, winds, and all final model parameters from this calibration for all additional simulations, updating only the weather inputs.

Baseline (1979–2005)

GCMs project climate starting in the past and then proceed into the future. As with many other studies that explore climate change impacts into the future (e.g., Barros et al. 2021; Clark et al. 2021; Heidari et al. 2021), we supplied FSim with GCM-based climate for both a future period and a recent historical period to fully capture a GCM’s expression of future climate while also capturing its bias by comparison to the actual observed climate. To understand this historical bias component, we first required simulation of a baseline climate scenario for comparison to the historical GCM-based climate described in the next section. To create the baseline, we conducted a single 10 000 iteration FSim simulation informed by 1979–2005 gridMET ERC values; in this case, we accepted the assumption that gridMET represents the “true” ERC values over 1979–2005. We chose the 1979–2005 time period because this overlaps with the standard historical period available for GCM-based climate described in the following section.

Historical (1979–2005)

Simulations for the historical climate period are informed by downscaled GCM-based climate over the 1979–2005 time period retrieved from the MACA-v2-METADATA downscaled climate dataset (Abatzoglou and Brown

2012). MACAv2-METDATA uses gridMET as the reference dataset for its downscaling algorithm. We calculated ERC in the same way as for the contemporary calibration and baseline periods, with the exception of adjustments we implemented to correct for “GCM drizzle.” “GCM drizzle” is a well-documented GCM phenomenon (Sun et al. 2006; Ahlgrimm and Forbes 2014) and is manifested in MACAv2-METDATA as an unrealistically high frequency of days with extremely light rain in the summer. Because this unrealistically suppresses ERC values, we adjusted the drizzle days by removing the lowest precipitation days from MACAv2-METDATA for the historical period until the number of drizzle days matched those in the gridMET data for the baseline period (i.e. the period we considered as the “true” values) for each month. In subsequent analyses, simulation results from the historical period were compared with simulation results from the baseline period to interpret GCM bias.

Future (2040–2069)

For this study we selected a mid-century period (2040–2069) under RCP8.5 high-warming climate change scenario to explore the impacts of significant climate change. While changes to the landscape resulting from disturbance are likely to occur, this period is not so far in the future that broad-scale vegetation changes such as biome shifts are expected. Retaining the same landscape for all simulations also has the advantage of isolating the effect of changes in climate on projected fire activity without these interacting with changes in vegetation to alter this signal. We made similar adjustments to correct for “GCM drizzle” in the ERC calculations, but the target number of drizzle days for the future period were altered by the ratio of unadjusted drizzle days in the future period to the historical period (Appendix 1). Total precipitation values were only trivially affected by this adjustment procedure. In subsequent analyses, simulation results from the future period (2040–2069) were compared to the historical period (1979–2005) to interpret projected changes within each GCM in the future.

Selection of GCMs for historical and future scenarios

FSim requires extensive computing power (for example, a single 10 000 iteration simulation run of FSim for our study region takes approximately 2 weeks to complete). To make computing more manageable for this study, we selected a subset of eight GCMs from the 18 available GCMs downscaled by MACAv2-METDATA (Abatzoglou and Brown 2012). We subjectively chose these eight GCMs to incorporate the broad range of variability in historical bias and future change in ERC-based “burn days,” the key climate threshold used by FSim to ignite and

spread fires (Appendix 2). In this evaluation, we defined historical bias for each GCM as the difference in average number of annual burn days between the historical and baseline periods, and we defined future change as the difference between each GCM’s future (2040–2069) and historical (1992–2005) periods. To evaluate our subset, we performed a post-hoc Kruskal–Wallis test for equality of distributions between the historical and future distribution of burn days for the 8-GCM subset and the full set of 18 available MACAv2-METDATA GCMs and found that there were no statistical differences between the two sets (Appendix 3), suggesting our selection of models reasonably represent all available climate projections. For each of the 8 GCMs selected, we conducted two separate FSim simulations, one using ERC values representative of the historical period (1979–2005) and one using ERC values representative of the future period (2040–2069).

Results

Contemporary calibration and baseline simulations

Our contemporary calibration (1992–2015) simulations produced averages of 0.43 and 0.87 large fires per year per 1000 km², with average sizes of 8.33 km² and 14.18 km², for the Central Coast and Southern Coast, respectively. Following standard FSim best practices, all numbers were calibrated well within the 70% confidence intervals of the observed fire records (Table 1). Seasonally, simulated median fire size and frequency of the contemporary calibration followed similar patterns as the corresponding observational record with some exceptions, notably an underrepresentation of median fire size during the fall and winter months in the Southern Coast, and a peak fire frequency lagged by about one month in both pyromes (Fig. 2).

In our baseline (1979–2005) simulation, monthly patterns of fire size and frequency held a similar pattern, but were lower than the 1992–2015 calibration period due to lower ERC during this time period (Fig. 2). Average annual burn probability for the baseline simulation were about four times higher for the Southern Coast at 0.0080 than the Central Coast at 0.0023. Burn probabilities are interpreted as percentages – for example, a burn probability of 0.0080 is equivalent to a 0.80% annual chance of a fire at that pixel. As expected, localized areas of high burn probability generally corresponded to places with historically high ignition density and fuel types with high rates of spread, such as the grass and grass-shrub dominated regions of the northeast and southeast sectors of the study area (Fig. 3). Grass and grass-shrub fuel types combined accounted for over 50% of the total study area and reported the highest average burn probability resulting from the baseline simulation (Fig. 4).

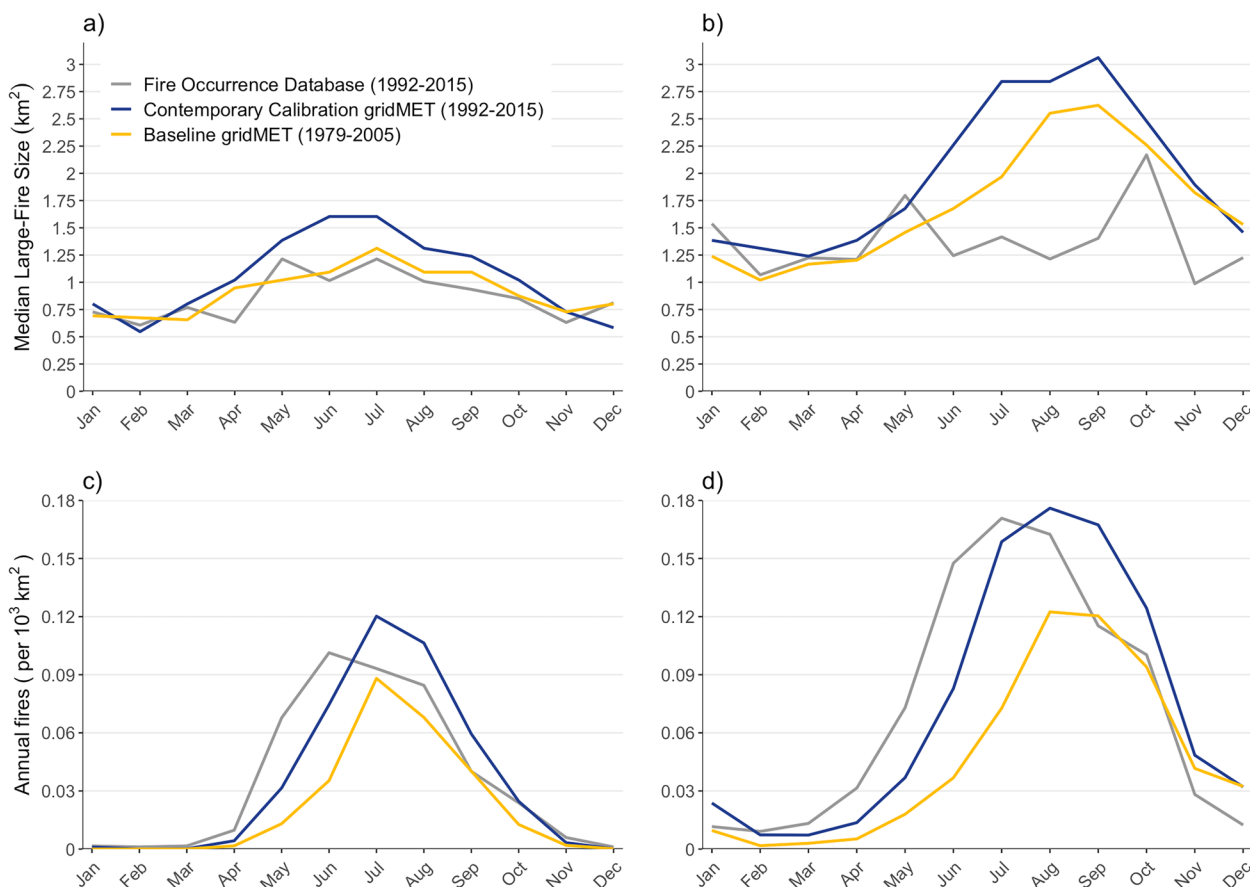


Fig. 2 Comparative monthly large-fire statistics from the observational fire occurrence database records and the baseline gridMET FSim runs. Median monthly large-fire size (km²) is shown for a) Central Coast and b) Southern Coast, and the monthly large-fire frequency (fires per 1000 km²) is shown for c) Central Coast and d) Southern Coast

Historical (1979–2005) and future (2040–2069) GCM-based simulations

When burn probability is averaged over the entire pyrome (hereafter referred to as landscape-wide burn probability), five simulations resulted in a future increase and three resulted in a decrease in the Central Coast pyrome, while six simulations resulted in a future increase and two resulted in a decrease in the Southern Coast pyrome (Fig. 5). Regardless of whether the simulation projected an overall increase or decrease, each individual simulation exhibited local spatial variability (Fig. 6). For example, even though the simulation based on GFDL-ESM2M projected the highest overall decrease of burn probability in the Southern Coast (Fig. 6c), some areas also had localized increases.

The spatial uncertainty was more pronounced for the GCM simulations that had an overall decrease of burn probability (e.g., bcc-csm1-1-m; Fig. 6a). In the Central Coast pyrome, three simulations projected an overall decrease in landscape-wide average burn probability. But, all three of these simulations simultaneously

agreed on a decrease in only 19.2% of all burnable pixels. In contrast, for the simulations that resulted in a landscape-wide increase in burn probability, 91.3% of the burnable pixels agreed across GCMs on an increase in burn probability. Across the study area, the majority of burnable areas had 5–6 simulations that all agreed on a burn probability increase, but few pixels had unanimous increase or decrease (Table 3; Fig. 7). In the Southern Coast, 89.41% of burnable pixels had 5–6 simulations that agreed on a burn probability increase; in the Central Coast, 74.55% of burnable pixels had 5–6 simulations that agreed on a burn probability increase.

Generally, relationships between large fire frequency and size were strong and related to burn probability, where larger and more frequent fires produced higher burn probabilities (Fig. 8). In the Central Coast, future changes in fire frequency ranged from -0.23 to $+0.36$ fires per year per 1000 km², while projected changes in fire size ranged from -3.19 km² to $+5.43$ km². In the Southern Coast, projected changes in ignition frequency ranged from -0.11 to $+0.41$ fires per year per

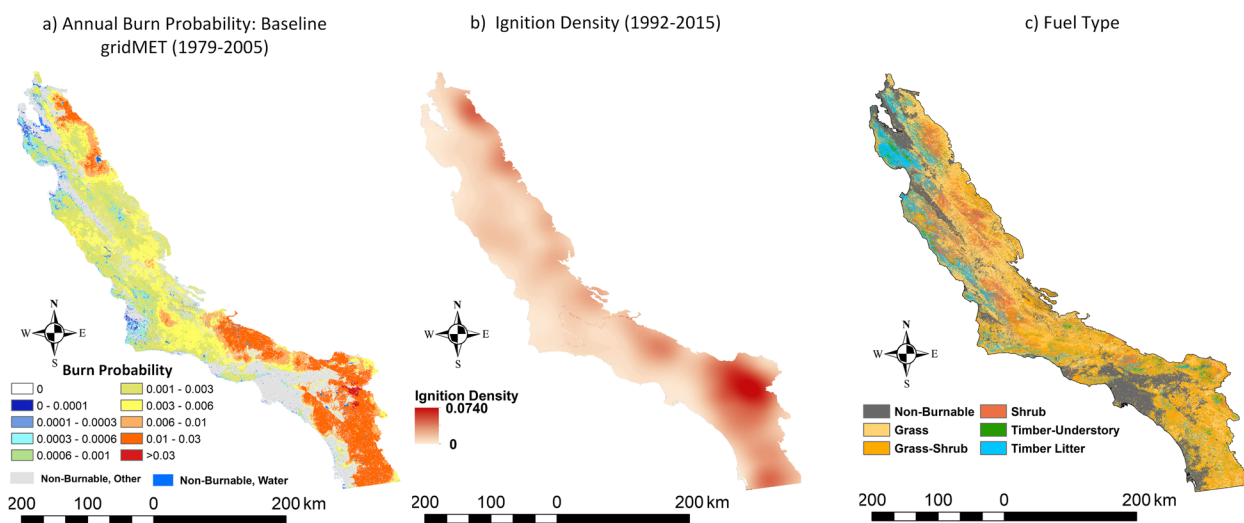


Fig. 3 Comparative maps showing a) the annual burn probability resulting from FSim simulations based on baseline gridMET (1979–2005); b) the ignition density grid based on the historical fire occurrence database (1992–2015); and c) the fire behavior fuel model (Scott and Burgan 2005) of the study area

1000 km², while projected changes in fire size ranged –3.07 km² to + 4.28 km². The grass and grass-shrub fuel types generally had the largest future increases in burn probability, while timber-litter generally had the least change, but the magnitude of those changes varied per the eight GCM-based simulations (Fig. 4).

Historical bias, defined as the difference between each GCM and the gridMET data for the historical period (1979–2005), was usually positive and large (up to 150% for burn probability and 55% for burn days), with the exception of those driven with HadGEM2-ES365 and MIROC5 in Central Coast (negative bias of less than

10% for burn days) and CanESM2 in Southern Coast (negative bias of 45% for burn probability) (Appendix 4). Bias in the average number of burn days was well correlated with bias in simulated landscape burn probability for both pyromes (adjusted R² = 0.89 and 0.94 for Central Coast and Southern Coast, respectively).

Future changes to ERC

To model fire ignition and spread, FSim model structure requires ERC burn days, which in turn are highly correlated with simulated burn probability; for our study, a future increase in burn days generally translated into

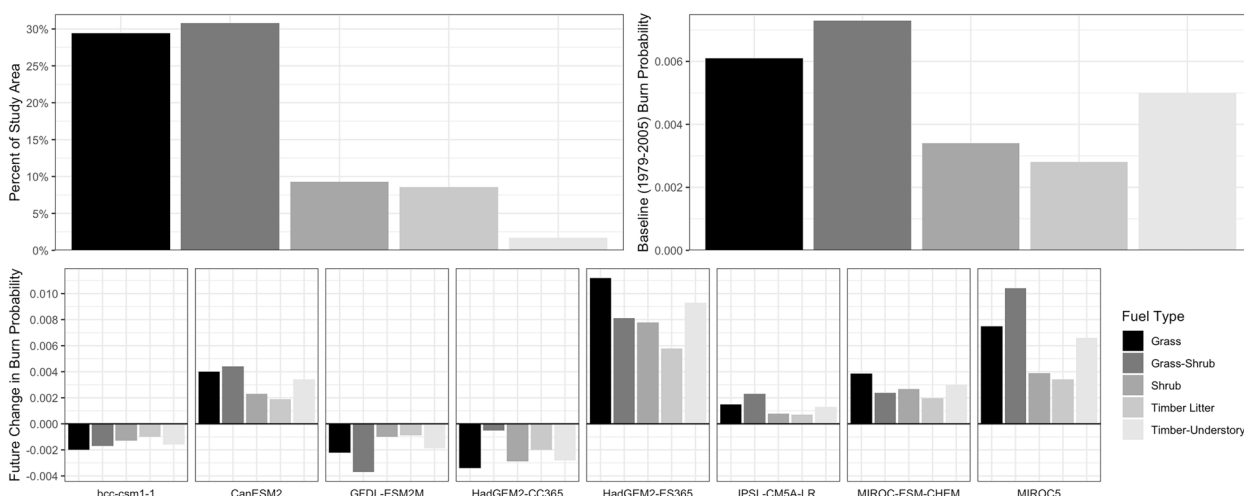


Fig. 4 Summary of results aggregated by fuel types (Scott and Burgan 2005) that were present in our study area: a) the percentage of the entire Southern California analysis area identified as each of five fuel types; b) the average burn probability for all pixels of each fuel type under the 1979–2005 baseline scenario; and c) for each GCM-based simulation, the change in burn probability between the future (2040–2069) and the baseline (1979–2005) scenarios by fuel type. All results reported here are summarized for the entire study area, i.e. they are not separated by pyrome

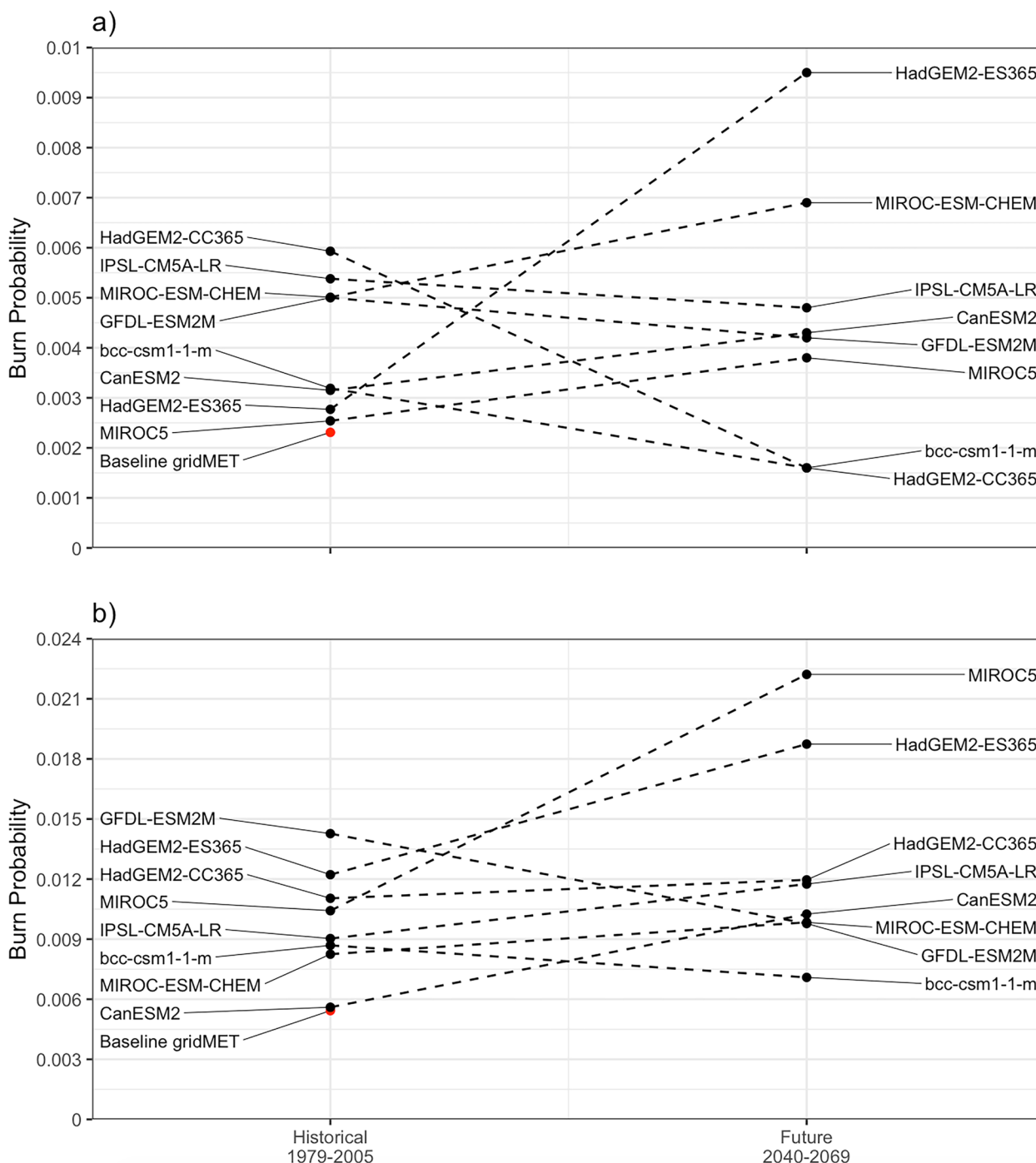


Fig. 5 Landscape burn probability simulated for the historical (1979–2005) and future (2040–2069) scenarios for **a** Central Coast and **b** Southern Coast. Dashed lines connect simulations based on the same GCM across both periods; red dots show the baseline gridMET burn probability

a future increase in burn probability (Fig. 9; adjusted $R^2=0.82$ and 0.92 for Central Coast and Southern Coast, respectively). But, there were notable exceptions to this rule—for example, Southern Coast simulations based on HadGEM2-CC365 projected a small increase of burn

probability despite a 5% decrease in burn days (Fig. 9). ERC is calculated primarily as a function of temperature, relative humidity, and precipitation – in general, warmer, drier, and less humid weather translates to lower fuel moisture and thus higher ERC. All GCMs that we

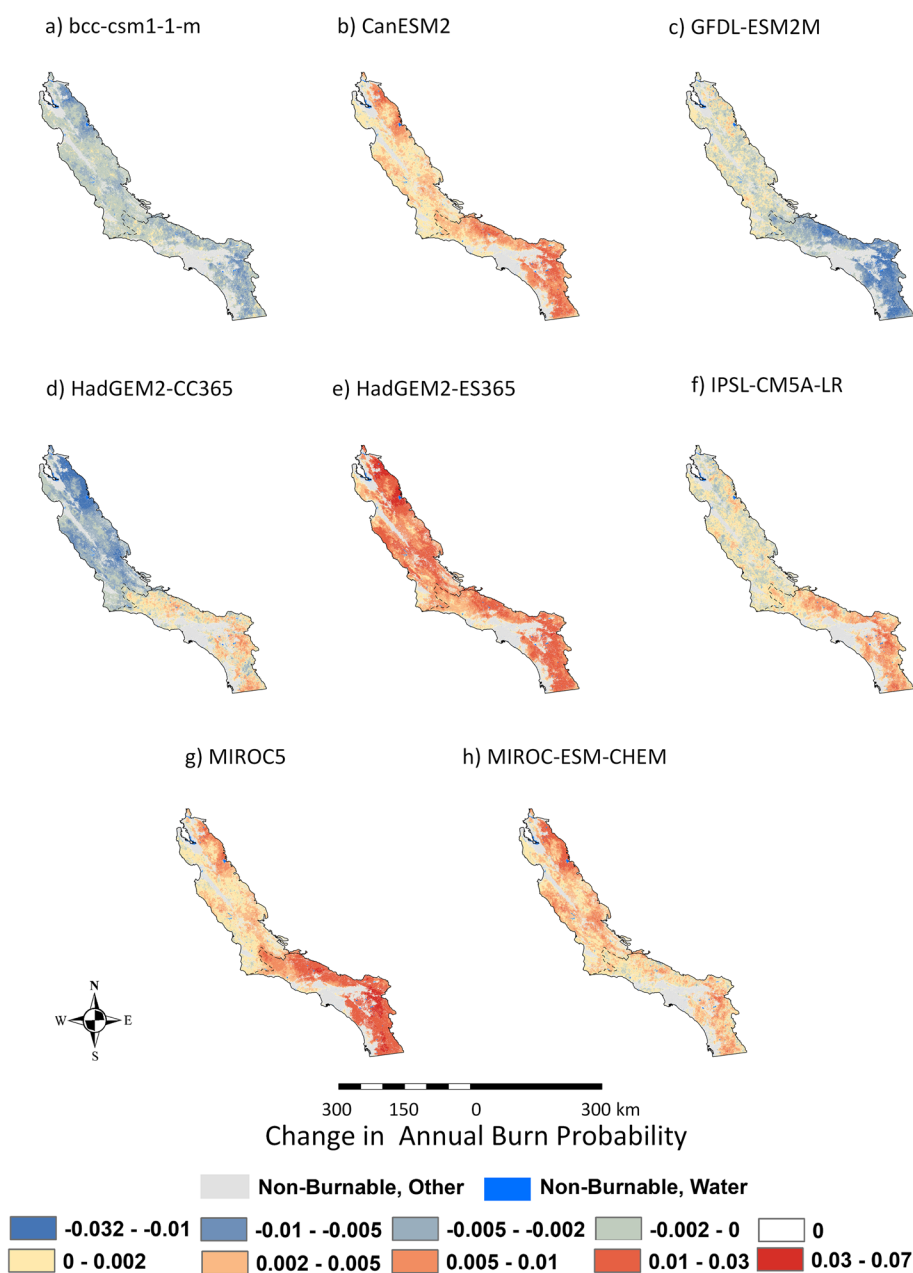


Fig. 6 Change in burn probability simulated from the historical (1979–2005) to future (2040–2069) periods for simulations based on each of 8 GCMs, a-h

Table 3 Percent of burnable area where 1–2, 3–4, 5–6, or 7–8 simulations agree on a burn probability increase, for each pyrome and for the combined study area. There were not any cases where no simulations had a burn probability increase, therefore 0 is omitted from table

	1–2	3–4	5–6	7–8
Central Coast	0.18%	23.69%	74.55%	1.58%
Southern Coast	0.05%	4.94%	89.41%	5.60%
Full Study Area	0.12%	15.22%	81.26%	3.40%

considered projected warmer futures, but projected precipitation and humidity varied (Fig. 10). Such wide variability is common for Southern California, where projections of future precipitation are notoriously uncertain (Neelin et al. 2013; Chang et al. 2015; Swain et al. 2018). Additionally, the magnitude of the projected climate change varied among the GCMs (Fig. 10), as did the seasonal distribution of changes (Appendix 5). In simulations based on bcc-csm1-1-m, for example, average annual temperature was projected to rise by nearly 2 °C

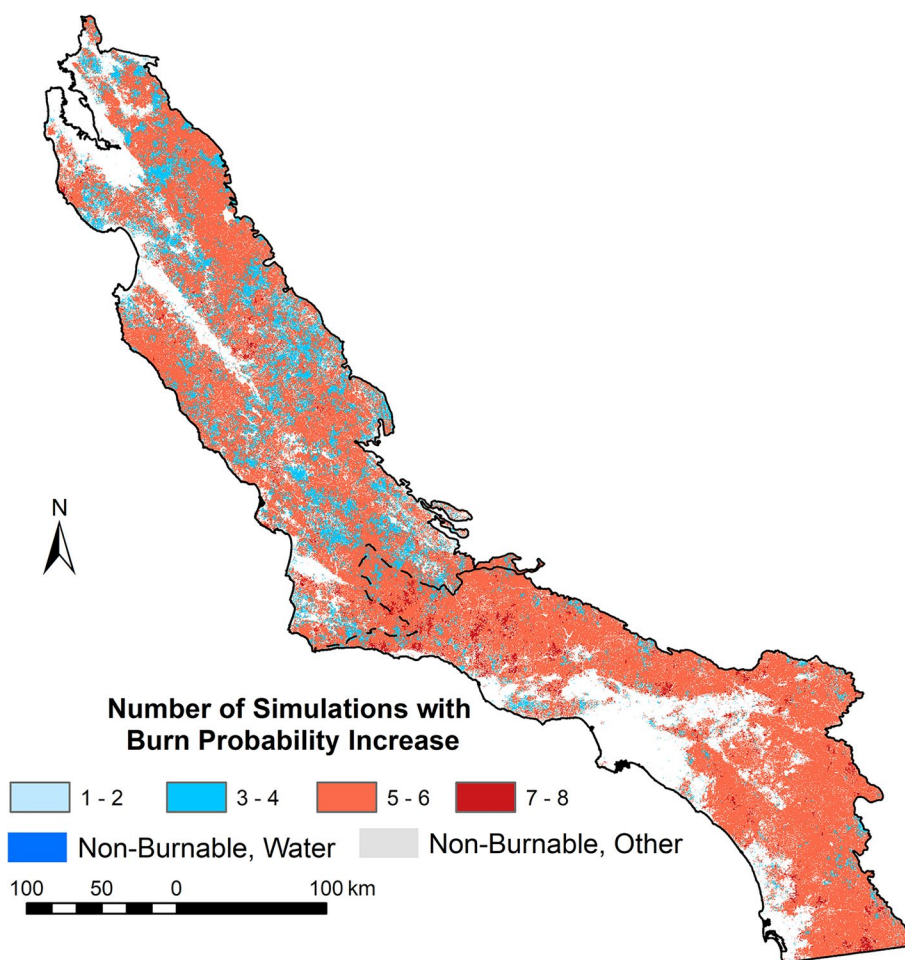


Fig. 7 Map showing areas where more than one simulation agree on a projected increase of burn probability from the historical (1979–2005) to future (2040–2069) periods

(near the lower limit of all projections we considered) in both pyromes (Fig. 10), but rainier winters and more humid summers resulted in reduced ERC and burn probability (Appendix 6). In the Central Coast, simulations based on HadGEM2-CC365 projected a decline in burn probability, despite projecting temperature increases of 2.7 °C, which was near the upper limit of the GCMs we considered. But, a 1% increase in relative humidity (largest humidity increase among all GCMs), combined with an average of 3 more rainy days per year, were sufficient to counteract the large temperature increase and corresponded with a reduced burn probability (Fig. 10).

Discussion

Simulation complexity

We found that while some simulations did suggest that fire activity could increase in the future, there is high uncertainty in where, when, and by how much these increases

occur. The complexity of future climate change on burn probability derives from the temporal variability of ERC and climatic variables (temperature, precipitation, and relative humidity) from which ERC is computed, the spatial variability of factors that contribute to fire growth (e.g., fuel types and topography), and interactions of both temporal and spatial variability. Wide variability in projections of climate change are not uncommon for Southern California, particularly for future precipitation projections which are notoriously uncertain in the region (Neelin et al. 2013; Chang et al. 2015; Swain et al. 2018). Seasonally, changes that occur in the winter, outside of Southern California’s primary fire season, can have less of an impact on fire than change occurring during the summer. For example, Central Coast simulations based on IPSL-CM5A-LR projected a warmer, drier, and less humid future but only a modest (5%) increase in burn probability (Fig. 10). However, the majority of the climatic changes occurred in the winter, when they

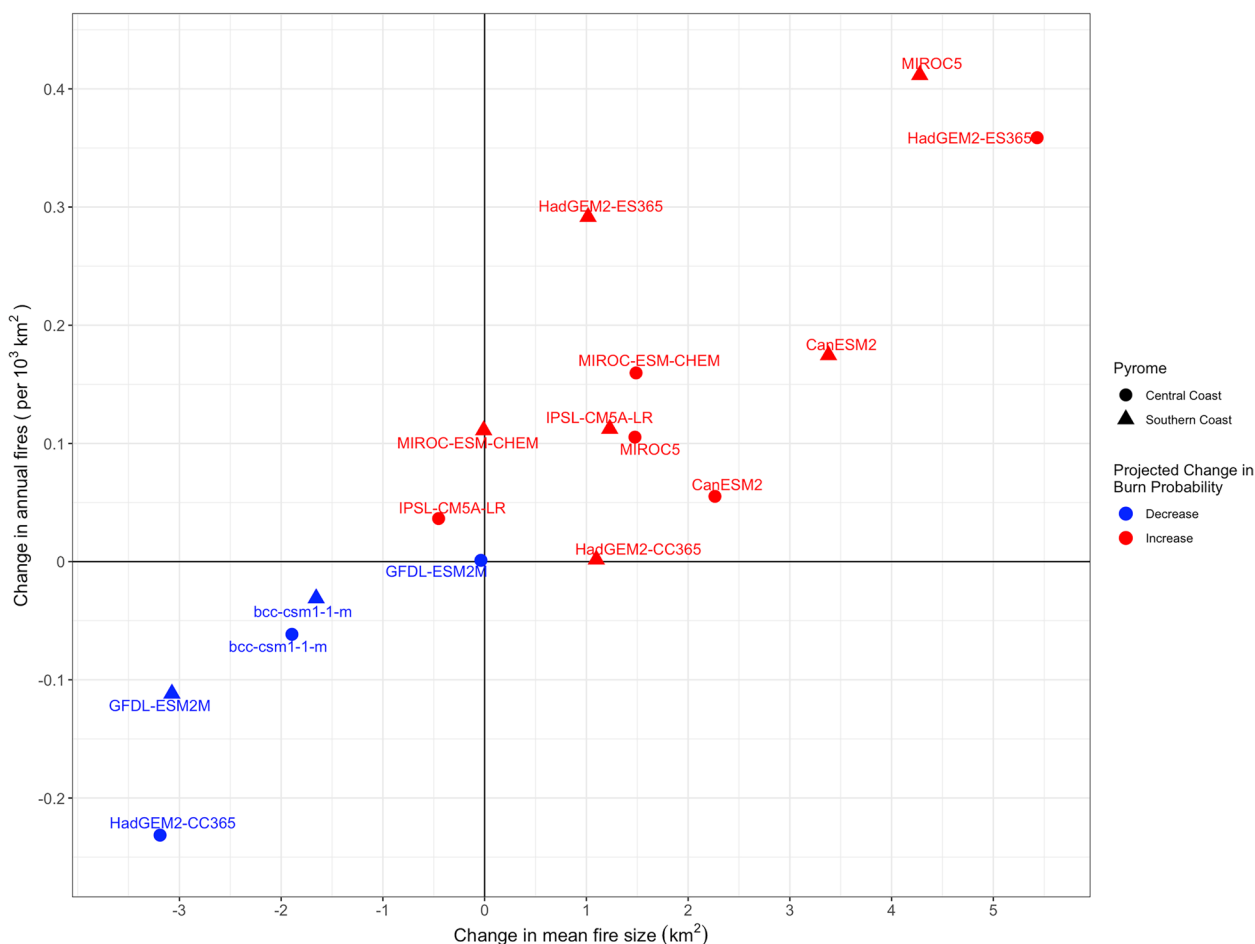


Fig. 8 Scatterplot showing the relationship between the change in mean fire size (km²) and annual fire frequency (fires per 1000 km²) from the historical (1979–2005) to future (2040–2069) periods

are less likely to impact fire, while summer was projected to become comparatively much more humid and rainier with relatively minor temperature increases (Appendix 5). Simulations based on CanESM2 were unique in that they projected an increase in burn probability for both pyromes despite also projecting an overall wetter and more humid future (Fig. 10). But, the majority of these changes occurred overwhelmingly in winter, outside of the main fire season, while in summertime, climate actually became more conducive to fire—in August, for example, projected temperatures increased by 3.8 °C and 4.5 °C for the Central and Southern Coast, respectively, while humidity decreased and precipitation remained unchanged (Appendix 5). Studies that rely on mean annual climate metrics cannot accurately capture these complexities, which are instrumental in making reasonable assumptions about shifts in fire regimes due to climate change. However, we did not account for seasonally lagged climate effects, such as the amount or timing of spring snowmelt, which can affect fuel dryness at high latitudes during the fire season (Westerling 2016).

Fire size and frequency

Burn probability derives from both the number of ignitions that are simulated and the final size of the fire as it grows over consecutive burn days (Fig. 8). FSim has a built-in suppression algorithm designed to stop fire growth after encountering more than two consecutive non-burn days if the ignition occurred in a non-timber fuel type, or more than seven consecutive burn days if ignition occurred in a timber fuel type. Therefore, once a fire ignites, the temporal variability of burn days, along with the ignition location, fuel type, topography, winds, and landscape characteristics, work together to determine the growth and final size of the fire. This contributes to the stochasticity that is a hallmark of FSim, allowing the model to simulate a more realistic version of fire behavior, spread, and containment than is possible with purely statistical models. It also reveals complexity in the relationship between burn days, ignition, fire size, and burn probability.

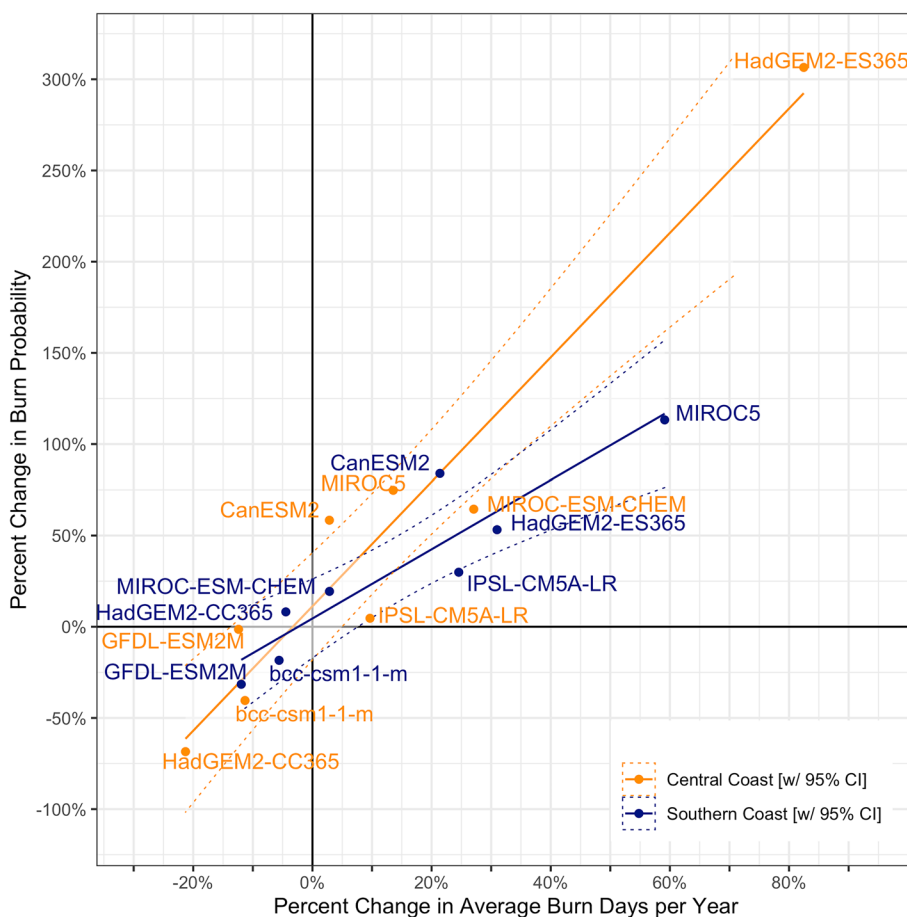


Fig. 9 The linear relationship between the percentage change in the average number of burn days per year (days exceeding the 80th percentile ERC) and the percentage change in annual burn probability, where projected change is the difference between the future period (2040–2069) and historical period (1979–2005) for each GCM

Recent modeling work by Ager et al. (2022) suggested that increases to fire size, rather than frequency, were more important for estimating future burned area, but our simulations did not unanimously support this hypothesis. For example, Central Coast simulations based on IPSL-CM5A-LR projected a decline in mean fire size of about 0.50 km² but an increase in ignition frequency, yet burn probability is still projected as a slight increase (Fig. 8). Similarly, Southern Coast simulations based on MIROC-ESM-CHEM projected an increase of fire frequency but negligible change to fire size, yet burn probability still had a projected increase of 20%. Clear relationships between size, frequency, and burn probability are also complicated by FSim’s spatial stochasticity. Relationships between size, frequency, and burn probability can be complex, because ignitions may be in different places in the different GCM simulations, combined with complicating factors of the seasonal distribution and magnitude of changes relative to specific aspects of the climate.

Fire activity is more than just climate

FSim simulations in this study reflected regional spatial patterns of the underlying contemporary fire record in Southern California, simulating high burn probability in regions that frequently experienced wildfire historically (Fig. 3), while spatial patterns in the future projections were modified by the magnitude and seasonality of interacting climate changes (Fig. 10). In reality, however, other factors will also influence the spatio-temporal patterns of fire in the future, in addition to climate. The spatial distribution of vegetation types was held constant in our simulations across all three timesteps, in order to isolate the effect of climate. However, vegetation distribution and conditions are unlikely to remain constant throughout the century as fire, drought, and insect and disease outbreaks catalyze long-term type shifts in California (Forrestel et al. 2011; Keeley and Brennan 2012; Syphard et al. 2019). A critical next step to modify additional versions of our work will be to incorporate potential future changes in vegetation (Harris et al. 2016). Vegetation shifts could

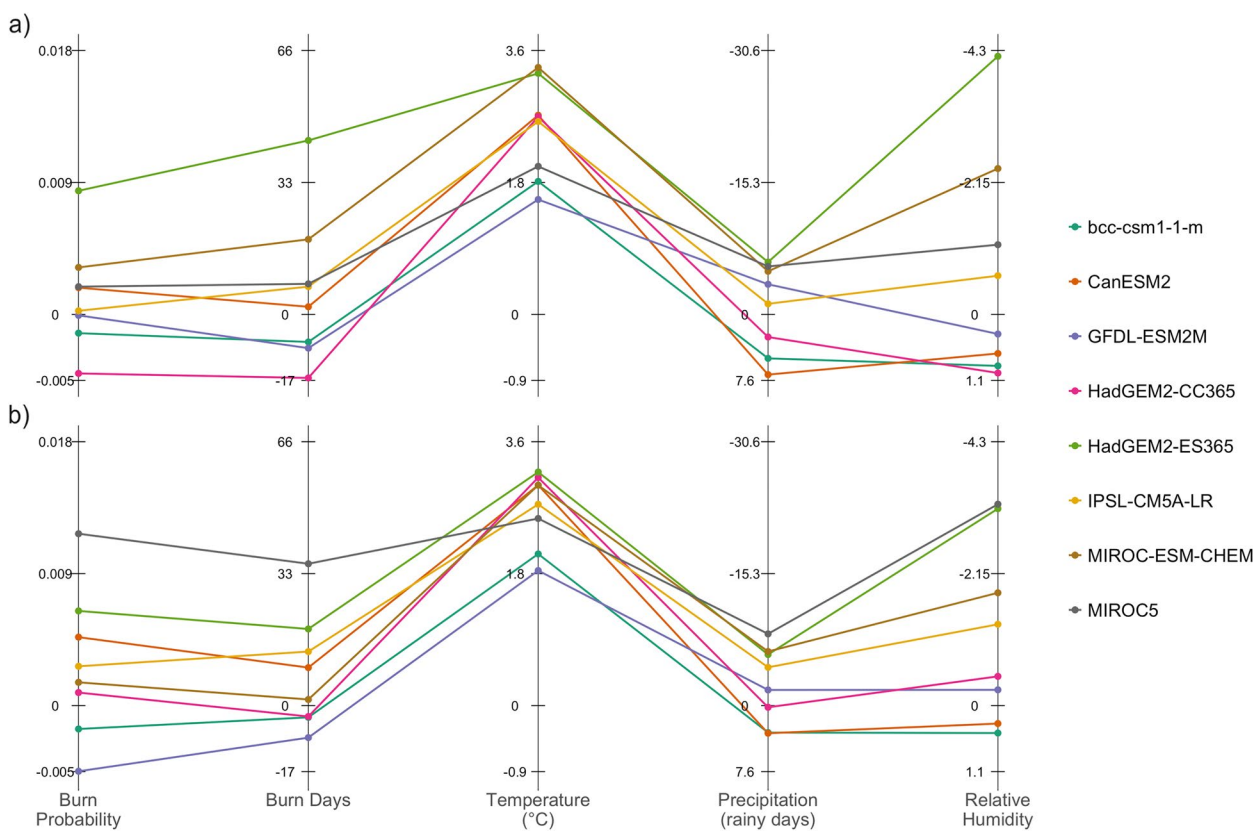


Fig. 10 The corresponding changes in annual burn probability, burn days per year, mean annual temperature, rainy days per year, and relative humidity from the historical (1979–2005) to future (2040–2069) period for a) Central Coast and b) Southern Coast. Note that y-axis scales for precipitation (rainy days per year) and relative humidity are inverted (i.e. negative changes, or drier conditions, are shown above the 0 line in order to map consistently with higher burn probability)

either moderate or exacerbate changes in fire probability depending on the type and direction of change. For example, Hurteau et al. (2019) showed that future projected area burned in the Sierra Nevada Mountains of California could be as much as 14% lower when modeled vegetation change is included in addition to climate change, because a warmer, drier climate would reduce the available biomass over the long term, while Parks et al. (2015) showed that fire could become self-limiting. Others have proposed that specific aspects of vegetation change will lead to more fire, such as the introduction of invasive species into previously unoccupied territory (Tortorelli et al. 2022). Climate-vegetation feedbacks are also critical. In our model structure, an increase in precipitation is most likely to decrease burn probability because this directly results in lower ERC values. However, it is possible that increased precipitation could lead to greater vegetation productivity, thereby increasing the availability of fuels to burn when droughts do occur (Ellis et al. 2021), and enhanced variability of wet and dry spells could then lead to periods of high productivity followed by periods of intense drought (Swain 2021). Similarly, the

interacting effects of precipitation and temperature in the future could change the underlying composition of forest biomass itself, which in turn has consequences for fire activity (Clark et al. 2017).

The timing of ERC change is particularly important for Southern California because the hot, dry summer fire season and the fall wind-dominated fire season often produce different fire effects (Jin et al. 2014; Keeley et al. 2021). Fast, dry downslope winds like the Santa Ana in the southern part of our study area (Raphael 2003; Guzman-Morales et al. 2016) and the Diablo winds in the northern part of our study area (Smith et al. 2018; Liu et al. 2021) are a major driver of autumn fires in California that have contributed to some of California’s most devastating wildfire disasters in recent years (Kolden and Abatzoglou 2018). Although future changes in winds were not explicitly considered in our study, projected changes in burn days could have had major implications for future simulated fire in the fall and winter by increasing or decreasing the chances of the model selecting days that both exceed FSim’s burn day threshold and also have high wind speeds. Santa Ana fires are not historically well

correlated with fuel moisture (Keeley et al. 2021), but a future increase in ERC heightens the possibility of high wind speeds coinciding with low fuel moisture, thereby increasing both the frequency of modeled ignitions and the ensuing rate of fire spread. However, just as vegetation is unlikely to remain constant, we cannot necessarily expect the occurrence of downslope winds to remain identical in the future. The few studies that have explored the future of Santa Ana winds agree that winds will become more concentrated in November–December, but may overall become less intense (Miller and Schlegel 2006; Guzman-Morales and Gershunov 2019).

ERC values calculated from the eight GCMs exhibited significant bias when compared to the gridMET-based ERC values during the historical period (1979–2005). These biases partly captured the uncertainty in the observation-based ERC values, as the observations are taken from a single location within each pyrome and may represent a single manifestation of climate in a chaotic weather system (Kreienkamp et al. 2012). Bias is common in modeling work and is not unique to our study, and it provides an opportunity to examine how present-day uncertainties relate to future projections. For example, a recent study for Southern California documented consistently positive historical bias in wildfire hazard predictors, with a 10-GCM ensemble median EDDI nearly 5 times that of their baseline gridMET EDDI (Fig. 6 in D. McEvoy et al. 2020a, b). Additional complications in our study arose by drawing climate information from single grid points. Whereas most GCMs are understood to reliably capture broad continental or global patterns, they exhibit much higher variability at the scale of a region, locality, or a single grid cell (Langenbrunner et al. 2015). However, FSim requires climate input from a single point, and averaging this climate over an entire pyrome, for example, may have dampened extremes and resulted in a more moderated weather stream than is realistic for any given pixel. For the large two-pyrome regional study area we considered, a pixel size of 270 m is fairly high-resolution and is sufficient to assess broad regional patterns; however, it is not sufficient to interpret highly local effects. Other limitations of the model are inability to capture micrometeorology (such as eddying of wind on the lee side of topography) and the potential for a cell to burn twice during a simulation year. In addition, future climate could produce no-analog fuel moisture (ERC) and wind conditions that are not captured by this study. Other sources of uncertainty we did not consider, but that will certainly continue to interact with climate to influence future fires, include changes to management practices (Williams and Abatzoglou 2016), population distribution (Syphard et al. 2019), Santa Ana wind

strength and seasonality (Guzman-Morales and Gershunov 2019), and the spatial pattern and cause of ignition (Balch et al. 2017).

Conclusion

Our study evaluated the effects of eight different climate change projections drawn from GCMs on mid-twenty-first century fire activity for Southern California. By incorporating each projection into a high-resolution spatial fire behavior simulator, we were able to describe a range of complexities related to the impact of climate alone on the direction, seasonality, and magnitude of future changes to fire activity. Our results are most useful for interpreting the differences in fire activity simulated with an array of potential mid-twenty-first century climate projections, under the RCP8.5 warming scenario only, and not as absolute predictions of fire activity in the future. Our study highlights the complexity we may expect to see in the future, and suggests that fire in the future will not follow one single homogeneous story. Examining this complexity is a critical step for understanding how fire models such as FSim can be appropriately used to prepare for future fire activity (Riley and Thompson 2017). Efforts to plan for future fire could leverage this complexity, for example, by following a model of resilient socio-ecological systems that are capable of thriving in a future that could have either more or less fires (McWethy et al. 2019). Future work that explores and resolves some of the limitations we mentioned in the discussion would be highly impactful for continuing to characterize the complexity of future fire.

Supplementary Information

The online version contains supplementary material available at <https://doi.org/10.1186/s42408-023-00179-2>.

Additional file 1: Appendix 1.

Additional file 2: Appendix 2.

Additional file 3: Appendix 3.

Additional file 4: Appendix 4.

Additional file 5: Appendix 5.

Additional file 6: Appendix 6.

Acknowledgements

We thank John Abatzoglou, Faith Ann Heinsch, and Karen Short for valuable support with data sharing and interpretation.

Authors' contributions

AWD and PG contributed equally as first-authors of the manuscript. AWD and PG designed the study, conducted all analyses, and wrote the manuscript. JBK helped design the analysis and contributed editorial input. TL contributed critical analytical expertise. KLR helped design the analysis and contributed fire modeling expertise and editorial input. LY helped design the analysis and contributed editorial input. The author(s) read and approved the final manuscript.

Funding

This work was supported by: the USDA Forest Service Western Wildland Environmental Threat Assessment Center in a joint venture agreement 19-JV-11261952–132 with Oregon State University; grant RC18-1034 from the US Department of Defense Strategic Environmental Research and Development Program (SERDP); the USDA Forest Service Missoula Fire Sciences Laboratory; and the Research Momentum Fund from the University of North Carolina Wilmington. Some of this work used the Extreme Science and Engineering Discovery Environment (XSEDE), which is supported by National Science Foundation grant number ACI-1548562. Western Wildland Environmental Threat Assessment Center, Strategic Environmental Research and Development Program, Research Momentum Fund at UNCW, USDA Forest Service Missoula Fire Sciences Laboratory, Extreme Science and Engineering Discovery Environment (XSEDE)

Availability of data and materials

The datasets used and/or analyzed during the current study are available from the corresponding author on reasonable request.

Declarations

Ethics approval and consent to participate

Not Applicable.

Consent for publication

Not Applicable.

Competing interests

The authors declare that they have no competing interests.

Author details

¹Department of Forest Ecosystems and Society, Oregon State University, Corvallis, OR 97331, USA. ²Department of Earth and Ocean Sciences, University of North Carolina Wilmington, Wilmington, NC 28403, USA. ³USDA Forest Service Western Wildland Environmental Threat Assessment Center, Corvallis, OR 97331, USA. ⁴Department of Geography & Atmospheric Science, University of Kansas, Lawrence, KS 66045, USA. ⁵USDA Forest Service Rocky Mountain Research Station, Missoula, MT 59808, USA. ⁶Department of Wildland Resources, Utah State University, Logan, UT 84322, USA.

Received: 30 May 2022 Accepted: 8 March 2023

Published online: 03 April 2023

References

- Abatzoglou, J.T. 2013. Development of gridded surface meteorological data for ecological applications and modelling. *International Journal of Climatology* 33: 121–131. <https://doi.org/10.1002/joc.3413>.
- Abatzoglou, J.T., and T.J. Brown. 2012. A comparison of statistical downscaling methods suited for wildfire applications. *International Journal of Climatology* 32: 772–780. <https://doi.org/10.1002/joc.2312>.
- Abatzoglou, J. T., and C.A. Kolden. 2013. Relationships between climate and macroscale area burned in the western United States. *International Journal of Wildland Fire* 22: 1003–1020. <https://doi.org/10.1071/WF13019>.
- Abatzoglou, J.T., and A.P. Williams. 2016. Impact of anthropogenic climate change on wildfire across Western US forests. *Proceedings of the National Academy of Sciences* 113: 11770–11775. <https://doi.org/10.1073/pnas.1607171113>.
- Ager, A.A., A.M.G. Barros, and M.A. Day. 2022. Contrasting effects of future wildfire and forest management scenarios on a fire excluded Western US landscape. *Landscape Ecology* 37: 1091–1112. <https://doi.org/10.1007/s10980-022-01414-y>.
- Ahlgrim, M., and R. Forbes. 2014. Improving the representation of low clouds and drizzle in the ECMWF model based on ARM observations from the Azores. *Monthly Weather Review* 142: 668–685. <https://doi.org/10.1175/MWR-D-13-00153.1>.
- Andrews, P.L., D.O. Loftsgaarden, and L.S. Bradshaw. 2003. Evaluation of fire danger rating indexes using logistic regression and percentile analysis. *International Journal of Wildland Fire* 12: 213–226. <https://doi.org/10.1071/WF02059>.
- Balch, J.K., B.A. Bradley, J.T. Abatzoglou, R.C. Nagy, E.J. Fusco, and A.L. Mahmood. 2017. Human-started wildfires expand the fire niche across the United States. *Proceedings of the National Academy of Sciences* 114: 2946–2951. <https://doi.org/10.1073/pnas.1617394114>.
- Barbero, R., J.T. Abatzoglou, N.K. Larkin, C.A. Kolden, and B. Stocks. 2015. Climate change presents increased potential for very large fires in the contiguous United States. *International Journal of Wildland Fire* 24: 892–899. <https://doi.org/10.1071/WF15083>.
- Barros, A.M.G., M.A. Day, H.K. Preisler, J.T. Abatzoglou, M.A. Krawchuk, R. Houtman, and A.A. Ager. 2021. Contrasting the role of human- and lightning-caused wildfires on future fire regimes on a Central Oregon landscape. *Environmental Research Letters* 16: 064081. <https://doi.org/10.1088/1748-9326/ac03da>.
- Battlori, E., M.A. Parisien, M.A. Krawchuk, and M.A. Moritz. 2013. Climate change-induced shifts in fire for Mediterranean ecosystems. *Global Ecology and Biogeography* 22: 1118–1129. <https://doi.org/10.1111/geb.12065>.
- Bradshaw, L.S., and E. McCormick. 2009. *FireFamily Plus User's Guide, version 4.0*. Boise: USDA Forest Service, Fire and Aviation Management. 282.
- Brey, S.J., E.A. Barnes, J.R. Pierce, A.L.S. Swann, and E.V. Fischer. 2021. Past variance and future projections of the environmental conditions driving Western U.S. summertime wildfire burn area. *Earth's Future* 9 (2): e2020EF001645. <https://doi.org/10.1029/2020EF001645>.
- Brown, E.K., J. Wang, and Y. Feng. 2021. US wildfire potential: A historical view and future projection using high-resolution climate data. *Environmental Research Letters* 16 (3): 034060. <https://doi.org/10.1088/1748-9326/aba868>.
- Chang, E.K.M., C. Zheng, P. Lanigan, A.M.W. Yau, and J.D. Neelin. 2015. Significant modulation of variability and projected change in California winter precipitation by extratropical cyclone activity. *Geophysical Research Letters* 42 (14): 5983–5991. <https://doi.org/10.1002/2015GL064424>.
- Clark, J.A., R.A. Loehman, and R.E. Keane. 2017. Climate changes and wildfire alter vegetation of Yellowstone National Park, but forest cover persists. *Ecosphere* 8: 301636. <https://doi.org/10.1002/ecs2.1636>.
- Clark, R.E., A.S. Hope, S. Tarantola, D. Gatelli, P.E. Dennison, and M.A. Moritz. 2008. Sensitivity analysis of a fire spread model in a chaparral landscape. *Fire Ecology* 4: 1–13. <https://doi.org/10.4996/fireecology.0401001>.
- Clark, S., G. Mills, T. Brown, S. Harris, and J.T. Abatzoglou. 2021. Downscaled GCM Climate Projections of Fire Weather over Victoria, Australia. Part 2. *International Journal of Wildland Fire* 30: 596–610. <https://doi.org/10.1071/WF20175>.
- Cohen, J.E., and J. D. Deeming. 1985. The National Fire-Danger Rating System: Basic Equations. Gen. Tech. Rep. PSW-82. Berkeley, CA: Pacific Southwest Forest and Range Experiment Station, Forest Service, U.S. Department of Agriculture. 16p. <https://doi.org/10.2737/PSW-GTR-82>.
- Cook, B.I., T.R. Ault, and J.E. Smerdon. 2015. Unprecedented 21st century drought risk in the American Southwest and Central Plains. *Science Advances* 1: e1400082. <https://doi.org/10.1126/sciadv.1400082>.
- Daly, C., M. Halbleib, J.I. Smith, W.P. Gibson, M.K. Doggett, G.H. Taylor, J. Curtis, and P.P. Pasteris. 2008. Physiographically sensitive mapping of climatological temperature and precipitation across the conterminous United States. *International Journal of Climatology* 28: 2031–2064. <https://doi.org/10.1002/joc.1688>.
- Diffenbaugh, N.S., D.L. Swain, and D. Touma. 2015. Anthropogenic warming has increased drought risk in California. *Proceedings of the National Academy of Sciences* 12: 3931–3936. <https://doi.org/10.1073/pnas.1422385112>.
- Dong, C., A.P. Williams, J.T. Abatzoglou, K. Lin, G.S. Okin, T.W. Gillespie, D. Long, Y. Lin, A. Hall, and G.M. MacDonald. 2022. The season for large fires in Southern California is projected to lengthen in a changing climate. *Communications Earth & Environment* 3: 1–9. <https://doi.org/10.1038/s43247-022-00344-6>.
- Dye, A.W., J.B. Kim, K.L. Riley. 2020. Spatial heterogeneity of winds during Santa Ana and Non-Santa Ana wildfires in Southern California with implications for fire risk modeling. *Heliyon* 6 (6): e04159. <https://doi.org/10.1016/j.heliyon.2020.e04159>.
- Ellis, T.M., D.M.J.S. Bowman, P. Jain, M.D. Flannigan, and G.J. Williamson. 2021. Global Increase in Wildfire Risk Due to Climate-Driven Declines in Fuel Moisture. *Global Change Biology* 28: 1544–1559. <https://doi.org/10.1111/gcb.16006>.

- Faivre, N. R., Y. Jin, M. L. Goulden, and J. T. Randerson. 2016. Spatial patterns and controls on burned area for two contrasting fire regimes in Southern California. *Ecosphere* 7: e01210. <https://doi.org/10.1002/ecs2.1210>.
- Finney, M.A. 2004. FARSITE: Fire Area Simulator - Model Development and Evaluation. Res. Pap. RMRS-RP-4. Ogden, UT: U.S. Department of Agriculture, Forest Service, Rocky Mountain Research Station. 47p. <https://doi.org/10.2737/RMRS-RP-4>.
- Finney, M.A. 2006. An Overview of FlamMap Modeling Capabilities. In Fuels Management—How to Measure Success: Conference Proceedings, Portland, OR, March 28–30, 2006, eds. P.L. Andrews and B.W. Butler. Proceedings RMRS-P-41, Fort Collins, CO: U.S. Department of Agriculture, Forest Service, Rocky Mountain Research Station, p. 213–220.
- Finney, M.A., C.W. McHugh, I.C. Grenfell, K.L. Riley, and K.C. Short. 2011. A simulation of probabilistic wildfire risk components for the continental United States. *Stochastic Environmental Research and Risk Assessment* 25: 973–1000. <https://doi.org/10.1007/s00477-011-0462-z>.
- Forrestel, A.B., M.A. Moritz, and S.L. Stephens. 2011. Landscape-scale vegetation change following fire in Point Reyes, California, USA. *Fire Ecology* 7: 114–128. <https://doi.org/10.4996/fireecology.0702114>.
- Gannon, C.S., and N.C. Steinberg. 2021. A global assessment of wildfire potential under climate change utilizing Keetch-Byram Drought Index and land cover classifications. *Environmental Research Communications* 3(3): 035002. <https://doi.org/10.1088/2515-7620/abd836>.
- Gao, P., A.J. Terando, J.A. Kupfer, J.M. Varner, M.C. Stambaugh, T.L. Lei, and J.K. Hiers. 2021. Robust projections of future fire probability for the conterminous United States. *Science of the Total Environment* 789: 147872. <https://doi.org/10.1016/j.scitotenv.2021.147872>.
- Goss, M., D.L. Swain, J.T. Abatzoglou, A.Sarhadi, C.A. Kolden, A.P. Williams, and N.S. Duffenbaugh. 2020. Climate change is increasing the risk of extreme autumn wildfire conditions across California. *Environmental Research Letters* 15: 094016. <https://doi.org/10.1088/1748-9326/ab83a7>.
- Guzman-Morales, J., and A. Gershunov. 2019. Climate change suppresses Santa Ana winds of Southern California and sharpens their seasonality. *Geophysical Research Letters* 46: 2772–2780. <https://doi.org/10.1029/2018GL080261>.
- Guzman-Morales, J., A. Gershunov, J. Theiss, H. Li, and D. Cayan. 2016. Santa Ana Winds of Southern California: Their climatology, extremes, and behavior spanning six and a half decades. *Geophysical Research Letters* 43: 2827–2834. <https://doi.org/10.1002/2016GL067887>.
- Harris, R.M.B., T.A. Remenyi, G.J. Williamson, N.L. Bindoff, and D.M.J.S. Bowman. 2016. Climate–vegetation–fire interactions and feedbacks: Trivial detail or major barrier to projecting the future of the Earth system? *Wiley Interdisciplinary Reviews: Climate Change* 7 (6): 910–931. <https://doi.org/10.1002/wcc.428>.
- Heidari, H., M. Arabi, and T. Warziniack. 2021. Effects of climate change on natural-caused fire activity in Western U.S. national forests. *Atmosphere* 12(8):981. <https://doi.org/10.3390/atmos12080981>.
- Hurteau, M.D., S. Liang, A.L. Westerling, and C. Wiedinmyer. 2019. Vegetation-fire feedback reduces projected area burned under climate change. *Scientific Reports* 9 (1): 2838. <https://doi.org/10.1038/s41598-019-39284-1>.
- Jin, Y., J.T. Randerson, N. Faivre, S. Capps, A. Hall, and M.L. Goulden. 2014. Contrasting controls on wildland fires in Southern California during periods with and without Santa Ana Winds. *Journal of Geophysical Research: Biogeosciences* 119: 432–450. <https://doi.org/10.1002/2013JG002541>.
- Keeley, J.E., J. Guzman-Morales, A. Gershunov, A.D. Syphard, D. Cayan, D.W. Pierce, M. Flannigan, and T.J. Brown. 2021. Ignitions explain more than temperature or precipitation in driving Santa Ana Wind fires. *Science Advances* 7: eabh2262. <https://doi.org/10.1126/sciadv.abh2262>.
- Keeley, J.E., H. Safford, C.J. Fotheringham, J. Franklin, and M. Moritz. 2009. The 2007 Southern California wildfires: Lessons in complexity. *Journal of Forestry* 107: 287–296. <https://doi.org/10.1093/jof/107.6.287>.
- Keeley, J.E., and T.J. Brennan. 2012. Fire-driven alien invasion in a fire-adapted ecosystem. *Oecologia* 169: 1043–1052. <https://doi.org/10.1007/s00442-012-2253-8>.
- Keeley, J.E., and A.D. Syphard. 2021. Large California wildfires : 2020 fires in historical context. *Fire Ecology* 17: 22. <https://doi.org/10.1186/s42408-021-00110-7>.
- Kolden, C.A., and J.T. Abatzoglou. 2018. Spatial distribution of wildfires ignited under katabatic versus non-katabatic winds in Mediterranean Southern California USA. *Fire* 1: 19. <https://doi.org/10.3390/fire1020019>.
- Kreienkamp, F., H. Huebener, C. Linke, and A. Spekat. 2012. Good practice for the usage of climate model simulation results - a discussion paper. *Environmental Systems Research* 1: 9. <https://doi.org/10.1186/2193-2697-1-9>.
- LANDFIRE. 2018. *Homepage of the LANDFIRE Project*. U.S. Department of Agriculture, Forest Service and U.S. Department of the Interior, U.S. Geological Survey. <http://www.landfire.gov/index.php>.
- Langenbrunner, B., J.D. Neelin, B.R. Lintner, and B.T. Anderson. 2015. Patterns of precipitation change and climatological uncertainty among CMIP5 models, with a focus on the midlatitude Pacific storm track. *Journal of Climate* 28: 7857–7872. <https://doi.org/10.1175/JCLI-D-14-00800.1>.
- Lenihan, J.M., D. Bachelet, R.P. Neilson, and R. Drapek. 2008. Response of vegetation distribution, ecosystem productivity, and fire to climate change scenarios for California. *Climatic Change* 87: 215–230. <https://doi.org/10.1007/s10584-007-9362-0>.
- Liu, Y.C., P. Di, S.H. Chen, X.M. Chen, J. Fan, J. DaMassa, and J. Avise. 2021. Climatology of Diablo winds in Northern California and their relationships with large-scale climate variabilities. *Climatic Dynamics* 56: 1335–1356. <https://doi.org/10.1007/s00382-020-05535-5>.
- Liu, Y., S.L. Goodrick, and J.A. Stanturf. 2013. Future U.S. wildfire potential trends projected using a dynamically downscaled climate change scenario. *Forest Ecology and Management* 294: 120–135. <https://doi.org/10.1016/j.foreco.2012.06.049>.
- Luković, J., J.C.H. Chiang, D. Blagojević, and A. Sekulić. 2021. A Later Onset of the Rainy Season in California. *Geophysical Research Letters* 48: 1–9. <https://doi.org/10.1029/2020GL090350>.
- Ma, W., L. Zhai, A. Pivovarov, J. Shuman, P. Buotte, J. Ding, B. Christoffersen, R. Knox, M. Moritz, R.A. Fisher, C.D. Koven, L. Kueppers, and C. Xu. 2021. Assessing climate change impacts on live fuel moisture and wildfire risk using a hydrodynamic vegetation model. *Biogeosciences* 18: 4005–4020. <https://doi.org/10.5194/bg-18-4005-2021>.
- Madadgar, S., M. Sadegh, F. Chiang, E. Ragno, and A. AghaKouchak. 2020. Quantifying increased fire risk in California in response to different levels of warming and drying. *Stochastic Environmental Research and Risk Assessment* 34: 2023–2031. <https://doi.org/10.1007/s00477-020-01885-y>.
- McEvoy, A., M. Nielsen-Pincus, A. Holz, A.J. Catalano, and K.E. Gleason. 2020a. Projected impact of mid-21st century climate change on wildfire hazard in a major urban watershed outside Portland. *Oregon USA. Fire* 3 (4): 1–24. <https://doi.org/10.3390/fire3040070>.
- McEvoy, D.J., D.W. Pierce, J.F. Kalansky, D.R. Cayan, and J.T. Abatzoglou. 2020b. Projected changes in reference evapotranspiration in California and Nevada: Implications for drought and wildland fire danger. *Earth's Future* 8 (11): 1–17. <https://doi.org/10.1029/2020EF001736>.
- McWethy, D.B., T. Schoennagel, P.E. Higuera, M. Krawchuk, B.J. Harvey, E.C. Metcalf, C. Schultz, C. Miller, A.L. Metcalf, B. Buma, A. Virapongse, J.C. Kulig, R.C. Stedman, Z. Ratajczak, C.R. Nelson, and C. Kolden. 2019. *Rethinking Resilience to Wildfire*. *Nature Sustainability* 2: 797–804. <https://doi.org/10.1038/s41893-019-0353-8>.
- Miller, N.L., and N.J. Schlegel. 2006. Climate change projected fire weather sensitivity: California Santa Ana Wind occurrence. *Geophysical Research Letters* 33: L15711. <https://doi.org/10.1029/2006GL025808>.
- Myers, N., R.A. Mittermeier, C.G. Mittermeier, G.A.B. Da Fonseca, and J. Kent. 2000. Biodiversity hotspots for conservation priorities. *Nature* 403 (6772): 853–858. <https://doi.org/10.1038/35002501>.
- Nauslar, N.J., J.T. Abatzoglou, and P.T. Marsh. 2018. The 2017 North Bay and Southern California Fires: A case study. *Fire* 1: 18. <https://doi.org/10.3390/fire1010018>.
- Neelin, J.D., B. Langenbrunner, J.E. Meyerson, A. Hall, and N. Berg. 2013. California winter precipitation change under global warming in the Coupled Model Intercomparison Project Phase 5 Ensemble. *Journal of Climate* 26: 6238–6256. <https://doi.org/10.1175/JCLI-D-12-00514.1>.
- Parks, S.A., L.M. Holsinger, C. Miller, and C.R. Nelson. 2015. Wildland fire as a self-regulating mechanism: The role of previous burns and weather in limiting fire progression. *Ecological Applications* 25: 1478–1492. <https://doi.org/10.1890/14-1430.1>.
- Peterson, S.H., M.A. Moritz, M.E. Morais, P.E. Dennison, and J.M. Carlson. 2011. Modelling long-term fire regimes of Southern California shrublands. *International Journal of Wildland Fire* 20 (1): 1–16. <https://doi.org/10.1071/WF09102>.

- Raphael, M.N. 2003. The Santa Ana Winds of California. *Earth Interactions* 7: 1–13. [https://doi.org/10.1175/1087-3562\(2003\)007%3c0001:TSAWOC%3e2.0.CO;2](https://doi.org/10.1175/1087-3562(2003)007%3c0001:TSAWOC%3e2.0.CO;2).
- Riley, K.L., J.T. Abatzoglou, I.C. Grenfell, A.E. Klene, and F.A. Heinsch. 2013. The relationship of large fire occurrence with drought and fire danger indices in the Western USA, 1984–2008: The role of temporal scale. *International Journal of Wildland Fire* 227: 894–909. <https://doi.org/10.1071/WF12149>.
- Riley, K.L., and R.A. Loehman. 2016. Mid-21st century climate changes increase predicted fire occurrence and fire season length, Northern Rocky Mountains, United States. *Ecosphere* 7: e01543. <https://doi.org/10.1002/ecs2.1543>.
- Riley, K.L., M.P. Thompson, J.H. Scott, and J.W. Gilbertson-Day. 2018. A model-based framework to evaluate alternative wildfire suppression strategies. *Resources* 7: 4. <https://doi.org/10.3390/resources7010004>.
- Riley, K.L., and M.P. Thompson. 2017. An uncertainty analysis of wildfire modeling. In *Uncertainty in natural hazards: modeling and decision support*, ed. K.L. Riley, M.P. Thompson, and P. Webley, 191–213. New York: Wiley and American Geophysical Union Books <https://doi.org/10.1002/9781119028116.ch13>.
- Scott, J.H. 2014. *Summarizing contemporary large-fire occurrence for land and resource management planning*. Pyrologix: Missoula, MT. http://pyrologix.com/wp-content/uploads/2015/01/Summarizing-historical-wildfire-occurrence_v0.1.pdf.
- Scott, J.H., and E.D. Reinhardt. 2001. Assessing crown fire potential by linking models of surface and crown fire behavior. Res. Pap. RMRS-RP-29. Fort Collins, CO: USDA Forest Service, Rocky Mountain Research Station.
- Scott, J.H., M.P. Thompson, and J.W. Gilbertson-Day. 2017. Exploring how alternative mapping approaches influence fire assessment and human community exposure to wildfire. *GeoJournal* 82: 201–215. <https://doi.org/10.1007/s10708-015-9679-6>.
- Scott, J.H., and R.E. Burgan. 2005. Standard fire behavior fuel models: a comprehensive set for use with Rothermel's surface fire spread model. Gen. Tech. Rep. RMRS-GTR-153. Fort Collins, CO: U.S. Department of Agriculture, Forest Service, Rocky Mountain Research Station. 72 p. <https://doi.org/10.2737/RMRS-GTR-153>.
- Scott, J.H., D. Helmbrecht, M.P. Thompson, D.E. Calkin, and K. Marcille. 2012. Probabilistic assessment of wildfire hazard and municipal watershed exposure. *Natural Hazards* 64: 707–728. <https://doi.org/10.1007/s11069-012-0265-7>.
- Short, K.C. 2015. Sources and implications of bias and uncertainty in a century of US wildfire activity data. *International Journal of Wildland Fire* 24: 883–891. <https://doi.org/10.1071/WF14190>.
- Short, K.C. 2017. Spatial wildfire occurrence data for the United States, 1992–2015 [FPA_FOD_20170508]. 4th Edition. Fort Collins, CO: U.S. Department of Agriculture, Forest Service Research Data Archive. <https://doi.org/10.2737/RDS-2013-0009.4>.
- Short, K.C., I.C. Grenfell, K.L. Riley, and K.C. Vogler. 2020. Pyromes of the conterminous United States. Fort Collins, CO: U.S. Department of Agriculture, Forest Service Research Data Archive. <https://doi.org/10.2737/RDS-2020-0020>.
- Smith, C., B.J. Hatchett, and M. Kaplan. 2018. A surface observation cased climatology of Diablo-like winds in California's Wine Country and Western Sierra Nevada. *Fire* 1 (2): 1–9. <https://doi.org/10.3390/fire1020025>.
- Srivastava, L., M. Hand, J.B. Kim, J.J. Sánchez, F. Lupi, C. Garnache, R.J. Drapek, and J.F. Quinn. 2020. How will climate change affect the provision and value of water from public lands in Southern California through the 21st century? *Agricultural and Resource Economics Review* 49: 117–149. <https://doi.org/10.1017/age.2020.3>.
- Sun, Y., S. Solomon, A. Dai, and R.W. Portmann. 2006. How often does it rain? *Journal of Climate* 19: 916–934. <https://doi.org/10.1175/JCLI3672.1>.
- Swain, D.L. 2021. A shorter, sharper rainy season amplifies California wildfire risk. *Geophysical Research Letters* 48 (5): 1–5. <https://doi.org/10.1029/2021GL092843>.
- Swain, D.L., B. Langenbrunner, J.D. Neelin, and A. Hall. 2018. Increasing precipitation volatility in twenty-first-century California. *Nature Climate Change* 8: 427–433. <https://doi.org/10.1038/s41558-018-0140-y>.
- Syphard, A.D., H. Rustigian-Romsos, M. Mann, E. Conlisk, M.A. Moritz, and D. Ackerly. 2019. The relative influence of climate and housing development on current and projected future fire patterns and structure loss across three California landscapes. *Global Environmental Change* 56: 41–55. <https://doi.org/10.1016/j.gloenvcha.2019.03.007>.
- Syphard, A.D. T.J. Brennan, and J.E. Keeley. 2019. Extent and drivers of vegetation type conversion in Southern California chaparral. *Ecosphere* 10:e02796. <https://doi.org/10.1002/ecs2.2796>.
- Thompson, M.P., J.H. Scott, P.G. Langowski, J.W. Gilbertson-Day, J.R. Haas, and E.M. Bowne. 2013. Assessing watershed-wildfire risks on National Forest System lands in the Rocky Mountain region of the United States. *Water* 5 (3): 945–971. <https://doi.org/10.3390/w5030945>.
- Tortorelli, C., J.B. Kim, N.M. Vaillant, K. Riley, A. Dye, T.C. Nietupski, K.C. Vogler, R. Lemons, M. Day, M.A. Krawchuk, and B.K. Kerns. 2022. Feeding the fire: annual grass invasion facilitates modeled fire spread across Inland Northwest forest-mosaic landscapes. *Ecosphere* 14: e4413. <https://doi.org/10.1002/ecs2.4413>.
- Vogler, K.C., A. Brough, C.J. Moran, J.H. Scott, and J.W. Gilbertson-Day. 2021. *Contemporary wildfire hazard across California*. Pyrologix: Missoula, MT. pyrologix.com/reports/Contemporary-Wildfire-Hazard-Across-California.pdf
- Westerling, A.L., and B.P. Bryant. 2008. Climate change and wildfire in California. *Climatic Change* 87: 231–249. <https://doi.org/10.1007/s10584-007-9363-z>.
- Westerling, A.L. 2016. Increasing Western US forest wildfire activity: Sensitivity to changes in the timing of spring. *Philosophical Transactions of the Royal Society B: Biological Sciences* 371: 20150178. <https://doi.org/10.1098/rstb.2015.0178>.
- Williams, A.P., and J.T. Abatzoglou. 2016. Recent advances and remaining uncertainties in resolving past and future climate effects on global fire activity. *Current Climate Change Reports*. 2: 1–14. <https://doi.org/10.1007/s40641-016-0031-0>.
- Williams, A.P., C.D. Allen, A.K. Macalady, D. Griffin, C.A. Woodhouse, D.M. Meko, T.W. Swetnam, S.A. Rauscher, R. Seager, H.D. Grissino-Mayer, J.S. Dean, E.R. Cook, C. Gangodagamage, M. Cai, and N.G. McDowell. 2013. Temperature as a potent driver of regional forest drought stress and tree mortality. *Nature Climate Change* 3 (3): 292–297. <https://doi.org/10.1038/nclimate1693>.
- Williams, A.P., J.T. Abatzoglou, A. Gershunov, J. Guzman-Morales, D.A. Bishop, J.K. Balch, and D.P. Lettenmaier. 2019. Observed impacts of anthropogenic climate change on wildfire in California. *Earth's Future* 7: 892–910. <https://doi.org/10.1029/2019EF001210>.
- Zigner, K., L.M.V. Carvalho, S. Peterson, F. Fujioka, G. Duine, C. Jones, D. Roberts, and M. Moritz. 2020. Evaluating the ability of FARSITE to simulate wildfires influenced by extreme, downslope winds in Santa Barbara, California. *Fire* 3 (29). <https://doi.org/10.3390/fire303002>.

Publisher's Note

Springer Nature remains neutral with regard to jurisdictional claims in published maps and institutional affiliations.